Heliyon 10 (2024) e38394

Contents lists available at ScienceDirect

Heliyon

journal homepage: www.cell.com/heliyon

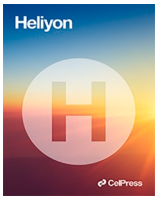

Research article

# Development of Methodology for molecular crystallization of Menthol

Ayesha Mushtaq [a,*], Muhammad Asif Hanif [a], Raziya Nadeem [a], Zahid Mushtaq [b]

[a] Department of Chemistry, University of Agriculture, Faisalabad, 38040, Pakistan
[b] Department of Biochemistry, University of Agriculture Faisalabad, 38040, Pakistan

ARTICLE INFO

*Keywords:*
Method development
Menthol
Crystallization
Food
Flavor
Mint
Crystals

ABSTRACT

Menthol, terpene alcohol with a strong minty, cooling odor and taste is highly popular in food, flavor, cosmetic and pharmaceutical industries. Crystallization of menthol from mint oil is a tedious process involving high cost and a much longer period. The present study has been undertaken to devise a new method with low input and with higher production rates. The crystallization of menthol was performed by the methods including Temperature programmed cooling process (TPCP); Short-path molecular fractional distillation (SPMFD) and Stripping crystallization (SC). About 99 % menthol contained in the mint oil was recovered during the crystallization process. The characterization techniques such as scanning electron microscopy (SEM) for surface morphology, x-ray diffraction (XRD) for crystal structure and crystallite size evaluation, and FTIR and Raman spectroscopy for analyzing the chemical nature of the crystals.

## 1. Introduction

The menthol finds extensive applications across the food, cosmetic, and pharmaceutical industries predominantly in the form of solid crystals [1]. It stands as the primary component in the composition of mint oils derived from *Mentha arvensis* (comprising 70 %–80 %) and *Mentha piperita* (comprising 50 %–60 %) [2], with recent research by Ref. [3] underscoring that *M. arvensis* contains double the menthol content in comparison to *M. piperita*. The conventional method for extracting mint oil is the steam distillation process, yielding approximately 1 %–5 % of oil, with variations depending on the mint species in use. Following a series of processing steps involving heating, filtering, and dewatering, the extracted oil is subjected to cooling within the temperature range of −5 °C to −10 °C. At these lower temperatures, menthol powder precipitates out of the oil. Subsequently, the dementholized mint oil (DMO) undergoes further cooling to reach −40 °C, causing an additional quantity of menthol

powder to precipitate [4]. For many decades, the majority of menthol crystal production units have used crystallization processes that involve subjecting mint essential oil to temperature-controlled procedures, which have either empirically established or derived from patented cooling techniques [5]. Some of these traditional crystallization processes can last up to thirty days and end at the final temperatures around −30 °C. Nevertheless, more recent advancements, such as the one described by Ref. [27], have significantly reduced processing times to a mere 48 h at −45 °C. These methods have a drawback of achieving a low menthol content due to the high solubility of menthol in other components of oil even at low temperatures. This de-mentholized oil is sold as a cheaper mint oil substitute, which is not economical. Therefore, traditional methods are in-efficient and only suitable for oils with over 50 % menthol

* Corresponding author.
*E-mail address:* ayesha_mushtaq123@yahoo.com (A. Mushtaq).

https://doi.org/10.1016/j.heliyon.2024.e38394
Received 4 June 2024; Received in revised form 23 September 2024; Accepted 23 September 2024
Available online 25 September 2024

content. In addition, these extended batch processing times in conventional methods result in excessive energy consumption, and the challenge persists regarding complete recovery of menthol crystals. There is a compelling and evident need to improve the conventional crystallization processes.

In this study, the production of menthol crystals was optimized by comparing three crystallization methods including short path molecular fractional distillation (SPMFD) combined with spray seeding crystallization (SSC), temperature programmed cooling process (TPCP), and stripping crystallization (SC). The SPMFD method combined SSC has been found to be the most effective among other methods for producing high-purity menthol. The SPFMD is an advanced distillation method which operates in high vacuum and isolate volatile compounds while minimizing thermal degradation, making it the best suited for heat sensitive compounds like menthol. Although this method necessitated precise control of working conditions and specialized equipment, these factors determine its significant advantages. The high level of control enables the production of pure menthol, avoiding the need for further purification. The initial investment in equipment may be greater, the efficiency and quality of results make it very cost-effective in the long run, especially in high-value applications where product purity is critical. Further the SSC method was employed to crystallize the liquid menthol fractions. By adding pure menthol seed crystals into the fractionated oil, SSC facilitates the controlled nucleation and uniform crystal growth, resulting in a higher yield of menthol crystals. This combination with SPMFD takes advantage of the capabilities of both approaches, improving the overall crystallization process. Alternative methods involving TPCP and SC were also employed to produce menthol crystals. The TPCP method uses gradual cooling, while SC approach depend on solvent removal to induce crystallization. By comparing these methods, this study determined that SPMFD combined with SSC is the best approach for the production of menthol crystals, offering high purity with reduced thermal degradation and confirming its higher product quality.

## 2. Materials and methods

### 2.1. Collection and pre-treatment of plants

Mint plants were collected from the field area at the Directorate of Farms, University of Agriculture Faisalabad, in mid-June when the flowers were in full bloom and lower leaves were starting to turn yellow [6]. The plants were hand-harvested before daylight. This time-period was chosen to prevent essential oil evaporation, which is caused by a rise in temperature and sun exposure. Harvesting in the morning provides for improved retention of essential oils, according to Ref. [7] who found that essential oils are better preserved during cooler portions of the day. Visual criteria were used to choose mature, healthy plants, which included bright green color, and no evident insect or disease damage. The stems were cut around 4–5 cm above the ground to promote regrowth of plants.

The mint plants were brought immediately to the laboratory after harvesting to prevent the components of essential oils from deteriorating. To avoid heat and light exposure, which can hasten oil loss, the plants were covered with damp towels and kept in cold, shady containers. The transit duration was kept to less than an hour, which is vital for preserving the chemical integrity of essential oils. The [8] has identified similar safety measures to lower temperature and light exposure during transportation as critical components in maintaining essential oil content. After that the rubbish, crushed branches, and brown leaves were manually removed from the raw material. The plant material was soaked in fresh water and gently agitated to remove any dust particles without causing damage to the plant surface [9]. Following washing, the plant material was air-dried in a shady area at room temperature for 30 min. Shaded drying is recommended to preserve plant material from deterioration caused by direct sunshine, which can harm sensitive components such as essential oils [10]. The 30-min drying interval allowed excess surface moisture to drain while keeping the plant's interior moisture level stable, which is required for efficient oil extraction. No further storage was needed, because extraction was performed directly after drying.

### 2.2. Extraction of EO from mint varieties

Hydro-distillation using a Clevenger type apparatus was used to extract essential oils from mint varieties. Ten kg of fresh plant material was soaked in 9 L of distilled water in a hydro-distiller. The tank containing plant material and water was heated by the burner at a temperature of 130 °C for 240 min. The setup was connected to the condenser and a separator to separate oil from water. At the end of distillation, the two phases were observed, an organic phase (essential oil) and aqueous phase (aromatic water). The EO was collected, dried under anhydrous $Na_2SO_4$, and stored in sealed vessels in the dark, at 4 °C, until used [11,12].

### 2.3. The yield of essential oils

The yield of essential oils extracted from different varieties of mint was expressed in grams per 100 g of fresh plant material. It was calculated according to equation (1) [13]:

$$Yield = \frac{Amount\ of\ extracted\ oil\ (g)}{Amount\ of\ fresh\ plant\ material\ (g)} \times 100 \ldots\ldots\ldots \quad (1)$$

### 2.4. Analysis of mint essential oil

The percentage menthol content in essential oil were analyzed by Gas Chromatograph (BK-GC7820), Biobase, China. The essential oil samples and standard menthol were analyzed with the following instrumental specifications; (a) Column pressure: 15 KPa (b) split-

less injection temperature: 200 °C (c) temperature of detector: 250 °C (d) temperature of oven: 40 °C (hold for 120 s) (e) $N_2$ carrier gas (f) $H_2$-air flame for combustion in detector (g) flame ionization detector (FID) [14].

### 2.5. Crystallization of menthol

The crystallization of menthol was performed by the following methods.

- Temperature programmed cooling process (TPCP)
- Short-path molecular fractional distillation (SPMFD) followed by improved seeding crystallization
- Stripping crystallization (SC)

### 2.6. Temperature-programmed cooling process

The temperature-programmed cooling process (TPCP) was performed using a lyophilizer (Christ Alpha 1–4 LD, Japan), operating under controlled temperature conditions. The lowest possible shelf temperature is around −55 °C. The 100g of purified mint oil was placed in the drying chamber of lyophilizer and gradually cooled to lower temperatures, causing the development of menthol crystals in each operation (Table 1). The chilling process was completed in three steps: (a) cooling at 14 °C, (b) 10 °C, (c) −5 °C. The process took 48 h to complete. A crystalline mass of menthol was produced at the end of 48 h along with the dementholized oil.

### 2.7. Stripping crystallization method

The experimental assembly used to conduct SC experiment consisted of a 250 mL sample vessel in chamber of large size fitted with a cooling jacket. The liquid nitrogen was injected to decrease the temperature of the chamber. The pressure in the chamber was lowered using a mechanical vacuum pump and turbomolecular pump in series. The big chamber was connected to a pressure gauge and temperature of the liquid mixture was monitored using a probe. The maximum working temperature and pressure of the apparatus were operable to −80 °C and 0.04Pa, respectively. At the start of experiments, 50 g of essential oil was taken in the sample chamber which was continuously stirred at 150 rpm using magnetic-driven motor. The cooling rate was 0.30 °C/min in the cooling jacket that was gradually decreased to 0.20 °C/min in the later stage. Vacuum pump was operated under controlled conditions to sustain three phase transformation conditions. The concentration of crystalized product was determined using GC-FID (Biobase, China).

### 2.8. Short-path molecular fractional distillation (SPMFD)

This process involves using high vacuum and converting essential oil components into vapors and condensing by sudden temperature decrease to form crystals [15]. The arrangement of the apparatus is shown in Fig. 1. The fractionating column, condenser, still pot, and collecting vials were all made of Pyrex glass so that the operation of the apparatus was completely visible. The length of the fractionating column was 14 mm. The still pot was a round bottom flask of 500 ml capacity. The heating mantle was used to provide the heat. A condenser was attached near the top of the column. A digital thermometer was used to indicate the temperature of boiling fractions. The oil was fractionated under a vacuum of 0 mmHg. The still was charged and a few small pieces of pumice were added to minimize bumping.

Two hundred ml of mint oil weighing 180 g was fractionated at a pressure of −760 mmHg. The sample was analyzed by GC-FID to contain 82 % free menthol. The still temperature was gradually raised, and the side heating was so adjusted that the column temperature was 1–2 °C below the vapor pressure at the still. The temperature was gradually raised and fractions with sharp melting points were collected. The process was continued until no more distillates came over and vapor temperature at the top of the column dropped rapidly. The present method is the improved form of previously used methods [16].

### 2.9. Seeding method

The seeding of pure menthol in the mint oil was also performed to produce molecular crystals of menthol. This method is the modified form of previously known seeding method [17]. The fractions separated in the SPMFD process were further subjected to the seeding crystallization. The analytical grade menthol crystals sourced from Sigma-Aldrich, were crushed manually to a fine powder to enhance crystal growth. Seeding was carried out as follows: 1) Seed crystals of pure menthol were added to the oil fractions in

**Table 1**
Temperature-programmed cooling of *Mentha* oil.

| Time (min) | Temp (°C) of the crystallization chamber |
|---|---|
| 0 | 30 |
| 5 min | 14 |
| 8 h | 10 |
| 16 h | −5 |
| 48h | Stop |

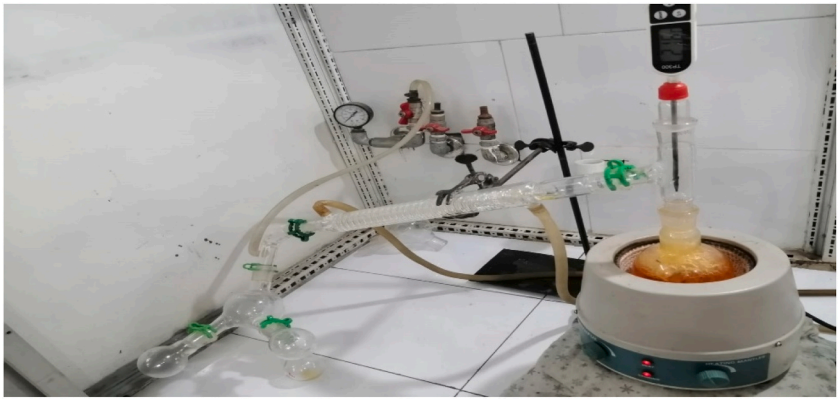

**Fig. 1.** The experimental setup of SPMFD of *Mentha* oil.

proportions of 10 %, 20 %, 30 %, 40 %, 50 %, 60 %, 70 %, 80 %, 90 %, and 100 %, 2) The resulting mixture was heated on a water bath, 3) A container was placed in the crystallization chamber of crystallizer, 4) the temperature of crystallizer was adjusted to −10 °C, 5) The solution containing oil fraction + seed crystals was atomized into a spray of droplets, into the container placed in the crystallizer, 6) The oil was allowed to cool for 30 min, 7) After 30 min, the container containing menthol crystals and dementholized oil was removed from the crystallizer 8) The mixture was left overnight at room temperature 9) The dementholized oil was evaporated leaving crystals of menthol. Similar process was repeated for each fraction.

### *2.10. Characterization of menthol crystals*

Menthol crystals were characterized by scanning electron microscopy (SEM), Raman spectroscopy, x-ray diffraction (XRD), and Fourier transform infrared spectroscopy (FTIR).

#### *2.10.1. Fourier transform infrared (FTIR) spectroscopic analysis*

Menthol crystals obtained from different fractions (F1, F2, F3, F4, F5, and residual fraction) along with the standard menthol crystals were characterized by using FTIR (Agilent Cary) spectrometer, USA, at a wavelength ranging from 600 $cm^{-1}$ to 4000 $cm^{-1}$. All the experiments were performed using 32 background scans and 32 sample scans, for each analysis. The analysis was carried out in triangular apodization, having a resolution of eight pixels per inch. The average of all spectra was used to build up the model [18].

#### *2.10.2. Scanning electron microscopy (SEM) analysis*

The morphological characteristics of menthol crystals produced from different fractions (F1, F2, F3, F4, F5, and residual fraction) along with standard (−)-menthol were studied by Nova Nano-SEM 450, FEI, Oregon, USA. The data was obtained in form of images taken at 200,000x (200 nm), 500,000x (500 nm), 50,000x (1 μm), 25000x (2 μm), 10,000x (5 μm), and 5000x (10 μm), using high voltage (10 KV) and width of 5 mm [19].

#### *2.10.3. Spectroscopic analysis of menthol crystals*

Raman spectral data acquisition from all samples was carried out using a Raman spectrometer (Pro-785 Peak Seeker; Agiltron, USA). The Pro-785 Peak Seeker utilizes a diode laser (785 nm) as the excitation source that delivers 40 mW laser power. The crystal sample was put on an Al substrate for the Raman spectral analysis. The CCD detector was used to record the Raman scattering and was cooled by a thermoelectric cooler to lessen the electrical noise. The Raman spectra for all the samples was performed from 200 to 1800 $cm^{-1}$. The pre-processing of spectra was carried out using MATLAB 7.2 (R2008b) and in house established protocols [20,21].

#### *2.10.4. Size distribution and zeta potential measurements*

The menthol crystals were characterized in terms of their zeta potential and size distribution using a Malvern Zeta-sizer Nano, ZSP UK [22].

## 3. Results and discussions

### *3.1. Yield of essential oil*

The essential oil obtained from *Mentha arvensis* leaves was yellow in color, with a very strong and persistent mint odor. The essential oil yield was observed to be 0.9 %. *Mentha piperita* yielded 44.6 % pale yellow-colored oil. In previous studies, the yield of essential oil obtained from mint ranged from 0.27 % to 3.02 % [23–25]. The differences in essential oil contents and chemical components are attributed to the factors involving phenophases, growth conditions, ecotype, climate, soil type, agriculture practices, genotype,

developmental stage of plant, agronomic conditions, plant part extracted, irradiance, photoperiod, relative humidity, and harvesting time [26].

### 3.2. Production of menthol crystals

Three methods including temperature programmed cooling process (TPCP), short-path molecular fractional distillation (SPMFD) followed by spray seeding crystallization **(**SSC), and stripping crystallization (SC) were employed for molecular crystallization of menthol.

#### 3.2.1. Temperature-programmed cooling process (TPCP)

Menthol rich mint oil containing 87.2 % menthol was subjected to temperature programmed cooling process. The percentage yield of menthol crystals was 61.2 % (Table 2). The results of current study are in close agreement with the previous studies [27,28]. The yield of menthol crystals through this method was lower than the original menthol content, as only 61.2 % menthol crystals were recovered from the mint oil containing 87.2 % menthol. This was probably due to the fact that menthol is highly soluble in menthone and other essential oil constituents, and even at low temperature a portion of menthol was retained in the residual oil [27].

It is evident from the above discussion that only oils with high menthol contents may be used to produce menthol crystals by this method. Since menthol content of the oil is seriously affected by the climatic conditions and varies from year to year. Moreover, the menthol content in the mint variety collected from different locations vary and usually is up to 50 % or less in most of varieties. Therefore, these varieties cannot be used as raw material to produce menthol crystals by this method. In addition, the melting point of the menthol crystals (i.e., 38 °C) was also lower than the USP specifications i.e., 43 °C. This indicated the presence of impurities (menthone and other constituents) on the surface of menthol crystals. According to previous reports the presence of trace amounts of impurities may adversely affect the quality and flavor of l-menthol [29–31]. Therefore, further methods of menthol purification were needed at additional costs in the production of purified menthol crystals.

#### 3.2.2. Short-path molecular fractional distillation (SPMFD)

The results of the SPMFD of mint oil are shown in Table 3. Short-path molecular fractional distillation was performed at 0 mmHg to separate menthol from other constituents present in the mint essential oil. This was because, the boiling point differences among menthol and other constituents in mint essential oil are very low (usually $\leq$7 °C) at atmospheric pressure, which makes the separation of menthol from other essential oil constituents difficult. In addition to this, some essential oil components (e.g., menthone) decompose rapidly when boiling at atmospheric pressure and cause darkening of mint oil and affects the properties of menthol also [32]. Moreover, according to previous literature, the resinification of essential oil was also found to slightly lowered at reduced pressures [33].

#### 3.2.3. Spray seeding crystallization (SSC)

The separated fractions were further subjected to the seeding process. The results of spray seeding method are shown in Table 4. Seed crystals have promoted the growth of menthol crystals. Stable menthol crystals were produced from F1 and F2 at the seed concentrations of 90 and 100 %. In case of F3, stable menthol crystals formed at the seed concentrations of 50 % and above. Fractions F4 and F5 produced stable menthol crystals at all concentrations except 10 %. This was probably due to high concentration of menthol in these fractions. The residual oil also produced menthol crystals, to a lesser extent. From the above results, it is clear that the SPMFD process separated different fractions at different temperatures. Fractions F4 and F5 were rich in menthol, the other fractions and residual oil also contained minor amounts of menthol along with other components. Stable menthol crystals were produced from all fractions, but the crystal yield varied due to the varying menthol content in the fractions. In view of preceding experimental results, it is seen that menthol can be obtained in crystalline form by SPMFD followed by spray seeding crystallization. The menthol-rich fractions F4 and F5 produced stable menthol crystals even at low seed crystal concentration. However, other low menthol fractions required a higher percentage of seed crystals to produce stable menthol crystals. In above method TPCP, the recovery of menthol crystals was only 61 %, a large volume of menthol was retained in the mother liquor, making that technique less suitable for the mint oils having low menthol content. But the SPMFD followed by the SSC method allowed the recovery of menthol from menthol rich fractions as well as fractions containing lesser amount of menthol. The method was simple as it required no expensive chemical or equipment cost. The crystallization process was also completed in short period of time. This method utilized mint oil containing less amount of menthol to produce menthol crystals. About 99 % menthol contained in the mint oil was recovered in this experiment. This process seems to be simple and may be expected to get a higher yield than the crystallization process.

**Table 2**
Yield of menthol crystals from TPCP process.

| | |
|---|---|
| Total oil used for crystallization | 250 g |
| Menthol content present in the oil | 82 % |
| By chilling crude *Mentha* oil | 126.03 g or 50.4 % |
| From remaining de-mentholized oil | 27.10 g or 10.8 % |
| Total yield of menthol crystals | 153.13 g or 61.2 % |

**Table 3**
Short-path molecular fractional distillation of mint essential oil.

| Fractions | Boiling point °C | Weight of fractions (g) |
|---|---|---|
| F1 | 21–23 | 5.9 |
| F2 | 32–35 | 4.6 |
| F3 | 36 | 16.8 |
| F4 | 37–39 | 31 |
| 'F5 | 42–50 | 51.6 |
| Residual oil | – | 18.5 |

**Table 4**
Production of menthol from spray seeding method.

| Conc. of seed crystals (%) | F1 | | F2 | | F3 | | F4 | | F5 | | R | |
|---|---|---|---|---|---|---|---|---|---|---|---|---|
| | Stability of crystals | %age yield | Stability of crystals | %age yield | Stability of crystals | %age yield | Stability of crystals | % age yield | Stability of crystals | %% age yield | Stability of crystals | % age yield |
| 10 | × | × | × | × | × | × | × | × | × | × | × | × |
| 20 | × | × | × | × | × | × | ✓ | 91 | ✓ | 90 | × | × |
| 30 | × | × | × | × | × | × | ✓ | 91 | ✓ | 93 | × | × |
| 40 | × | × | × | × | × | × | ✓ | 96 | ✓ | 93 | × | × |
| 50 | × | × | × | × | × | × | ✓ | 97 | ✓ | 98.9 | × | × |
| 60 | × | × | × | × | ✓ | 7 | ✓ | 97 | ✓ | 98.9 | × | × |
| 70 | × | × | × | × | ✓ | 11 | ✓ | 97 | ✓ | 98.9 | × | × |
| 80 | × | × | × | × | ✓ | 11 | ✓ | 97 | ✓ | 98.9 | ✓ | 2 |
| 90 | ✓ | 4 | ✓ | 13 | ✓ | 11 | ✓ | 97 | ✓ | 98.9 | ✓ | 3 |
| 100 | ✓ | 4.5 | ✓ | 15 | ✓ | 11 | ✓ | 97 | ✓ | 98.9 | ✓ | 3 |

### *3.2.4. Stripping crystallization*

The percentage of menthol crystallized from mint oil is shown in (Table 5). SC process was continued till −80 °C and 0.04 Pa. The results obtained showed that it was more difficult to purify essential oil with lower initial concentrations of menthol. The solid/liquid crystallization and crystal washing are not required for SC as no solvent was added to sample feed. In this regard, SC is a clean technology. The separation and purification of menthol from other components present in essential oil is a costly and difficult process. However, this separation process is very important for chemical industries. In general, 40–75 % cost accounts to separation processes in industry. Stripping crystallization (SC) involves combined processes of melt crystallization and vaporization via a series of three-phase transformations to produce crystalline product. SC involves the reducing of pressure and lowering of temperature to simultaneously vaporized and crystallized product. SC process was kept continued until the complete elimination of liquid phase and appearance of pure crystals in the sample feed. The vapor produced at lower pressure was condensed to remove.

## *3.3. Characterization of menthol crystals*

The physical and chemical properties of menthol crystals were studied by SEM, FTIR, Raman Spectroscopy, and XRD analysis.

### *3.3.1. SEM analysis of menthol crystals*

SEM images of standard menthol crystals showed a highly expended accordion-like structure containing randomly aggregated folded sheets arranged in 3-dimensional architecture. Few hemi-spherical to rectangular shaped particles can also be visualized near to aggregated sheets **(**Fig. 2a**)**. SEM images of menthol have not been described in the previous literature; however, SEM images of graphene oxide flakes have shown similar morphology [34]. The SEM images of menthol crystals produced from fractions F1, F2, F3, F4, F5, and residual fraction showed that particle size of crystals ranged from 200 nm to 10 μm. In F1 menthol crystals, mostly rectangular nanoparticles (and in some cases oval to cylindrical shaped particles) with smooth surfaces, arranged evenly in a crystalline pattern have been observed. Inter-crystalline pores can also be seen near the particles (Fig. 2b). In F2 menthol crystals, particles of almost semi-rectangular shape (in some cases pseudo spherical or cubic) with rough surface were observed (Fig. 2c). Few inter-granular spaces were also found. In case of F3 menthol crystals semi-spherical to rectangular-shaped particles arranged in a uniform pattern with scattered agglomerated needles have been observed (Fig. 2d). In F4 menthol crystals, spherical to rectangular particles with a smooth surface were uniformly aligned in a crystalline pattern with inter-crystalline voids (Fig. 2e). SEM images of F5 menthol

**Table 5**
Percentage (%) of menthol crystalized from total menthol in essential oil using SC process.

| *Sr#* | *Mentha* variety | Percentage (%) of menthol in essential oil | Percentage (%) of menthol crystalized from total menthol in essential oil |
|---|---|---|---|
| *1* | MA | 87.20 | 93.23 |
| *2* | MP | 44.64 | 75.76 |

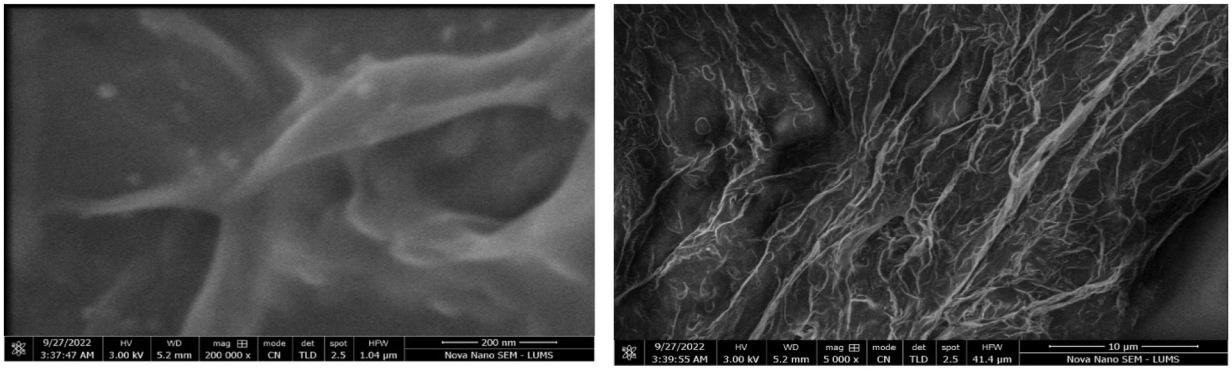


(a): SEM images of standard menthol crystals taken at (a) 200nm

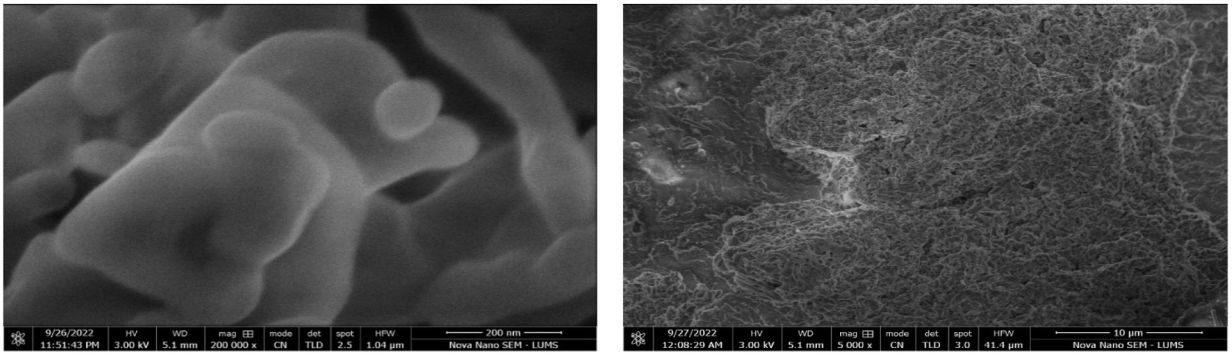


(b): SEM images of F1 menthol crystals taken at (a) 200nm and (b) 10 µm

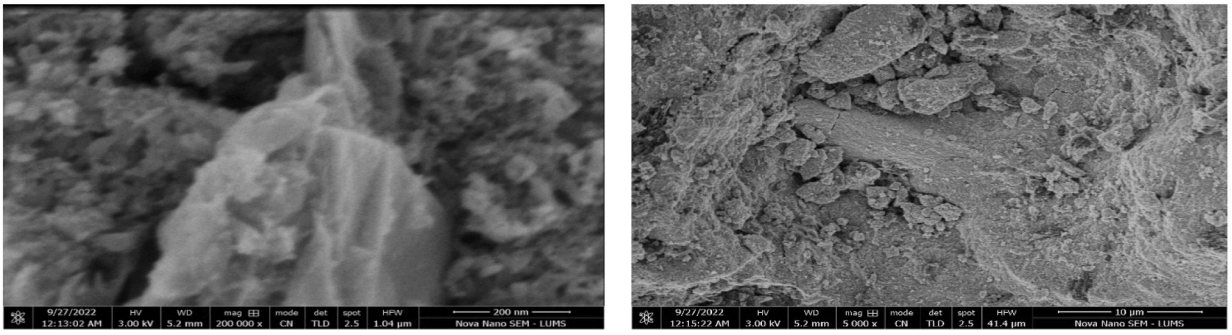


(c): SEM images of F2 menthol crystals taken at (a) 200nm and (b) 10 µm

**Fig. 2.** (a): SEM images of standard menthol crystals taken at (a) 200 nm and (b) 10 µm (b): SEM images of F1 menthol crystals taken at (a) 200 nm and (b) 10 µm (c): SEM images of F2 menthol crystals taken at (a) 200 nm and (b) 10 µm (d): SEM images of F3 menthol crystals taken at (a) 200 nm and (b) 10 µm (e): SEM images of F4 menthol crystals taken at (a) 200 nm and (b) 10 µm (f): SEM images of F5 menthol crystals taken at (a) 200 nm (b) 10 µm (g): SEM images of residual menthol crystals taken at (a) 200 nm (b) 10 µm.

crystals showed semi-rectangular shaped particles with smooth surfaces mostly uniformly aligned with inter-crystalline spaces (Fig. 2f). The menthol crystals produced from residual oil showed rectangular shape particles arranged in uniform pattern (Fig. 2g). Empty spaces near the particles were also found.

The SEM analysis showed that menthol crystals produced in this study differ in morphology from standard menthol crystals. Standard menthol crystals showed aggregated sheets like structure, while menthol crystals produced in this study showed the presence of nanoparticles of mostly rectangular shapes arranged in a uniform pattern. These results revealed that spray-seeding crystallization method reduced the particle size of menthol crystals. This reduction in size of menthol crystals would be helpful in the practical application of crystals in drug delivery system. As we know that menthol is a widely used drug in medication, food, and esthetic applications [35]. In general, drug particles with a small size and narrow distribution (high surface area) are desirable to manipulate

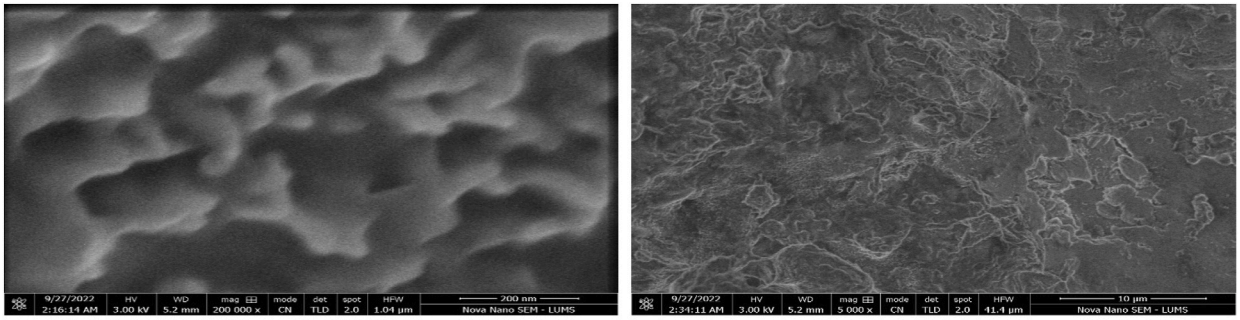


(d): SEM images of F3 menthol crystals taken at (a) 200nm and (b) 10

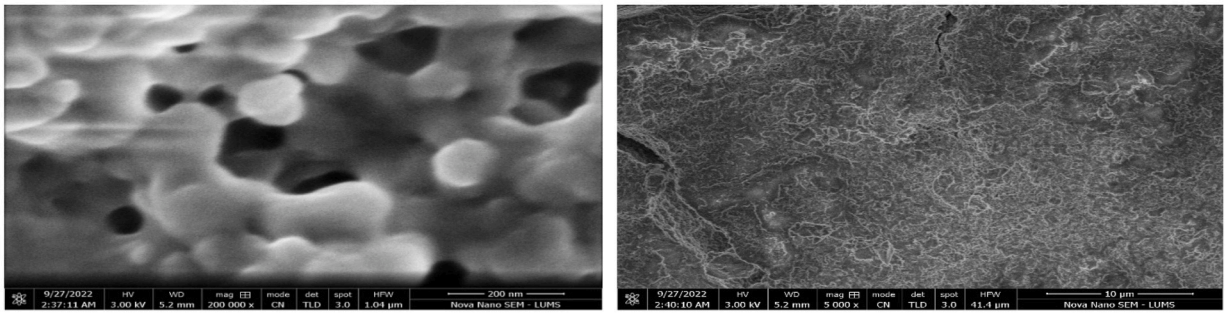


(e): SEM images of F4 menthol crystals taken at (a) 200nm and (b) 10 µm

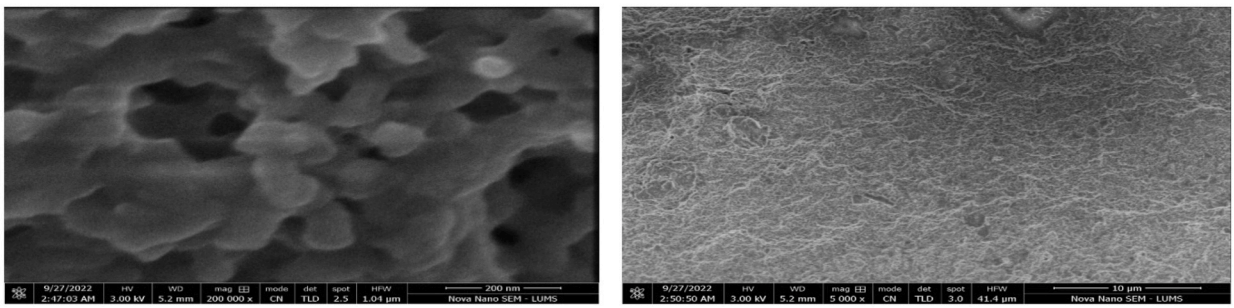


(f): SEM images of F5 menthol crystals taken at (a) 200nm (b) 10 µm

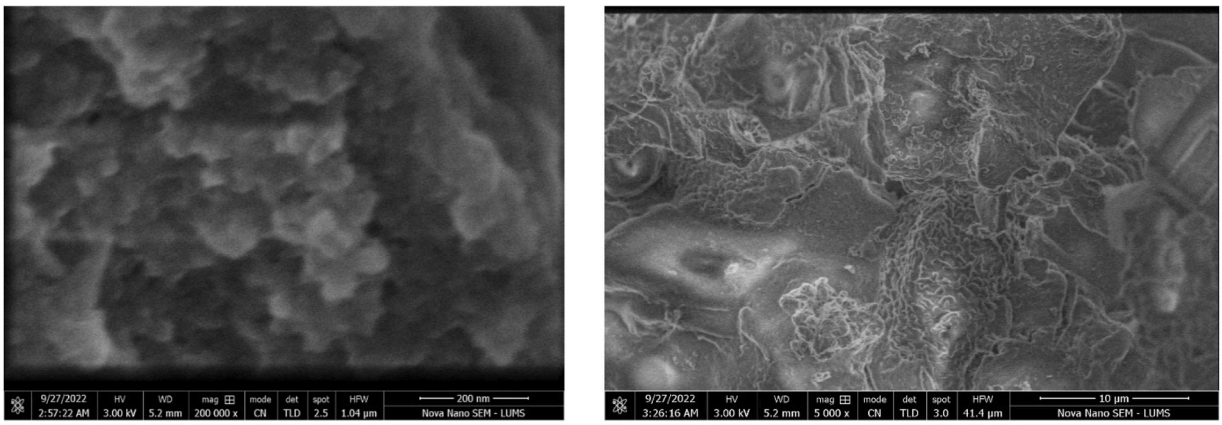


(g): SEM images of residual menthol crystals taken at (a) 200nm (b) 10 µm

**Fig. 2.** (*continued*).

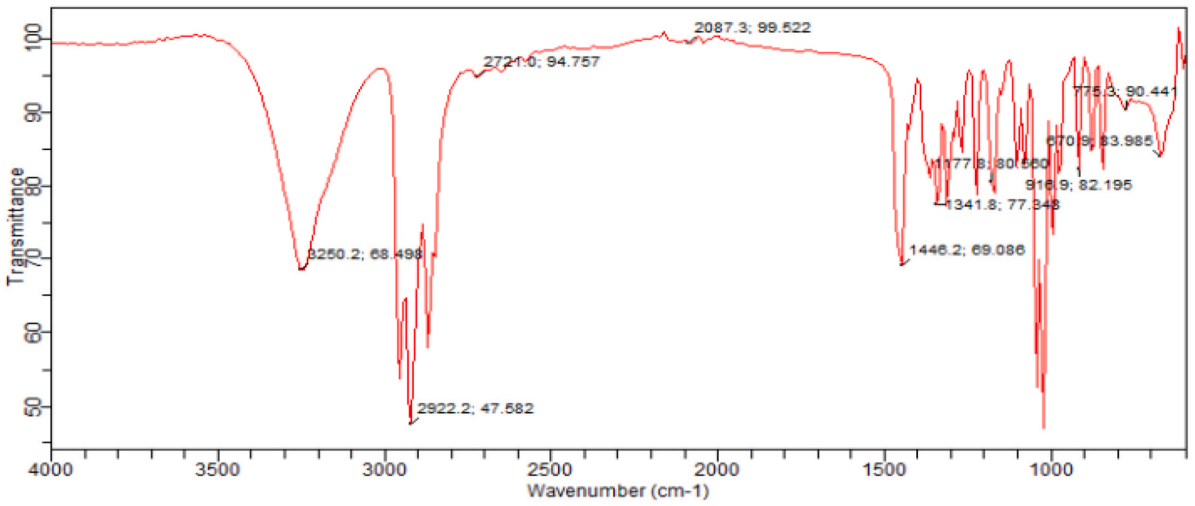


**(a):** FTIR analysis of standard menthol crystals

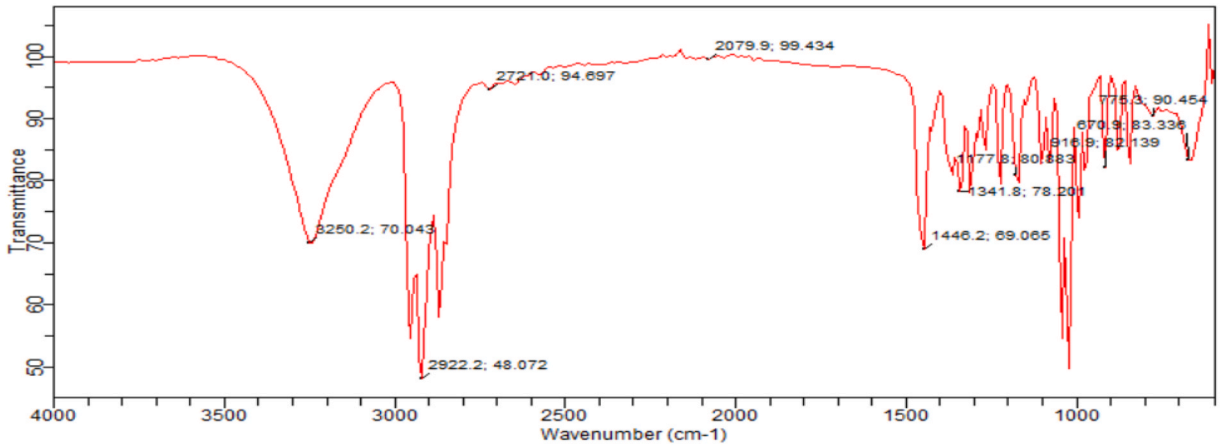


**(b):** FTIR analysis of menthol crystals produced from F1

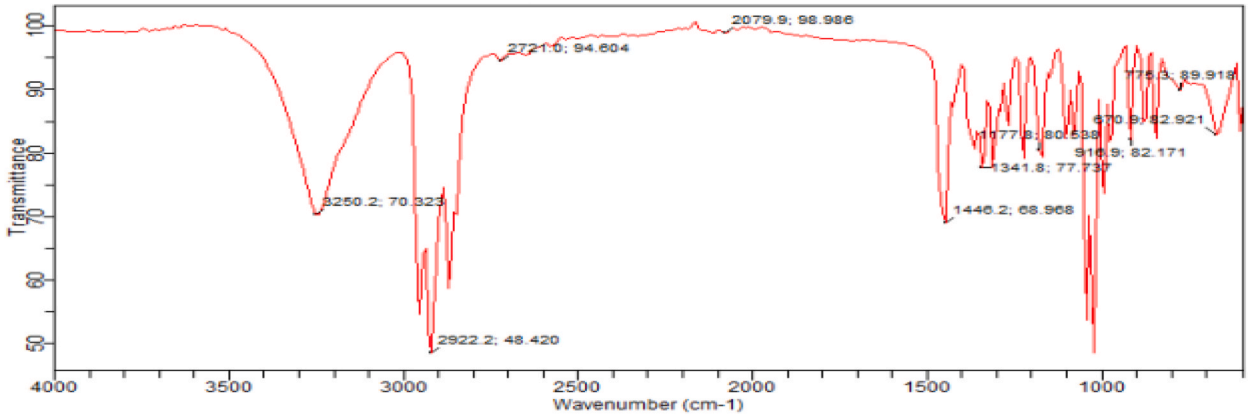


**(c):** FTIR analysis of menthol crystals produced from fraction F2

**Fig. 3.** (a): FTIR analysis of standard menthol crystals (b): FTIR analysis of menthol crystals produced from F1 (c): FTIR analysis of menthol crystals produced from fraction F2 (d): FTIR analysis of menthol crystals produced from fraction F3 (e): FTIR analysis of menthol crystals produced from F4 fraction (f): FTIR analysis of menthol crystals produced from fraction F5. .

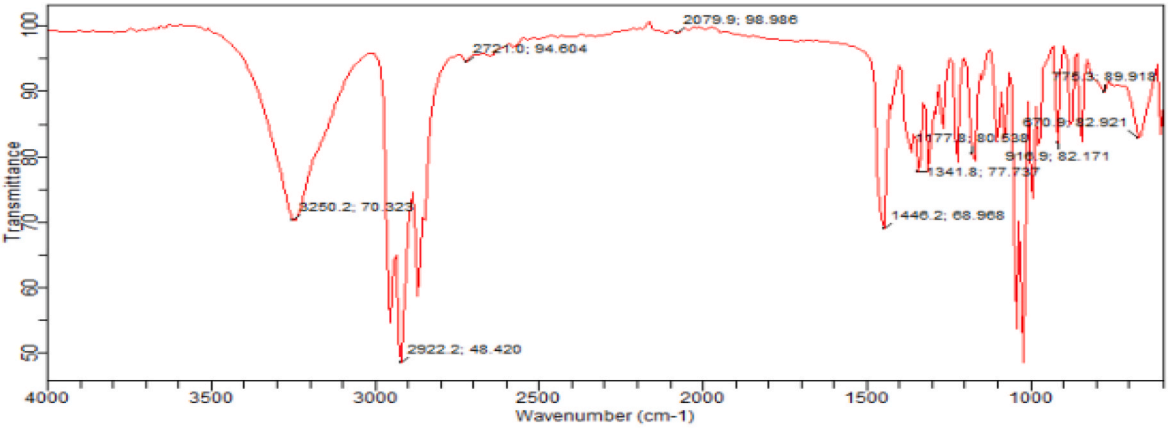


**(d):** FTIR analysis of menthol crystals produced from fraction F3

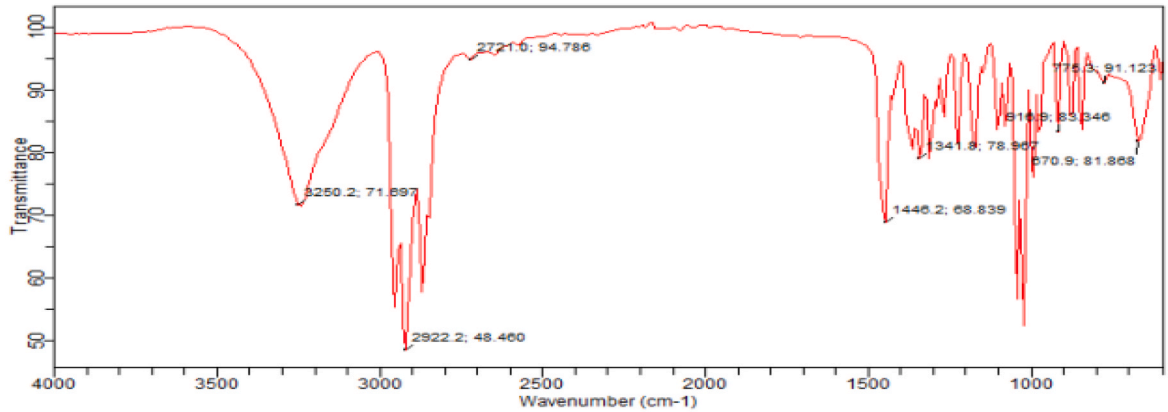


**(e):** FTIR analysis of menthol crystals produced from F4 fraction

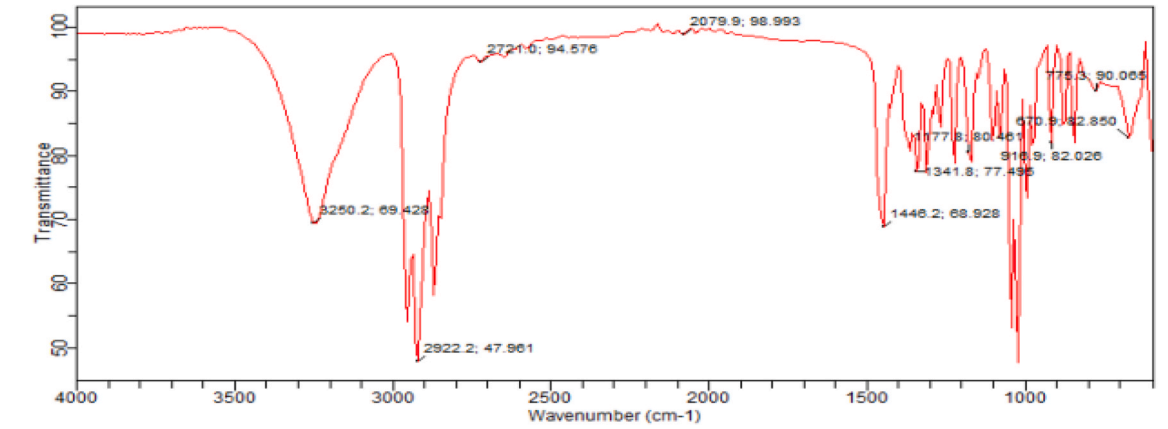


**(f):** FTIR analysis of menthol crystals produced from fraction F5

**Fig. 3.** (*continued*).

their delivery rate. The particle size reduction of drugs is mainly through thermal degradation, which is not possible with menthol crystals as they are thermally unstable [36]. This alternative method yielded stable micronized menthol crystals, that could be used more efficiently in drug delivery systems [37]. Further, chemical analysis (FTIR and RAMAN spectroscopy) analysis was performed to check whether there were changes in chemical composition of crystals or not.

| | | | Size (d.nm): | % Intensity: | St Dev (d.n... |
|---|---|---|---|---|---|
| Z-Average (d.nm): | 209.5 | Peak 1: | 228.4 | 96.6 | 159.2 |
| PdI: | 0.449 | Peak 2: | 5397 | 3.4 | 311.5 |
| Intercept: | 0.946 | Peak 3: | 0.000 | 0.0 | 0.000 |
| Result quality : | Good | | | | |

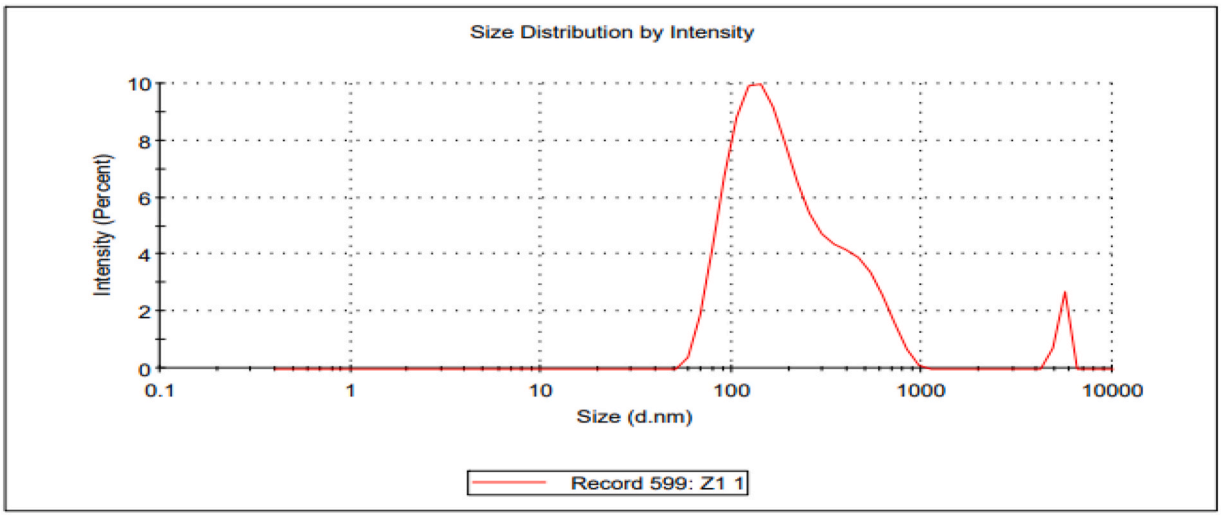


**(a):** Size distribution analysis of menthol crystals

| | | | Mean (mV) | Area (%) | St Dev (mV) |
|---|---|---|---|---|---|
| Zeta Potential (mV): | -28.4 | Peak 1: | -28.4 | 100.0 | 5.06 |
| Zeta Deviation (mV): | 5.06 | Peak 2: | 0.00 | 0.0 | 0.00 |
| Conductivity (mS/cm): | 0.0322 | Peak 3: | 0.00 | 0.0 | 0.00 |
| Result quality : | Good | | | | |

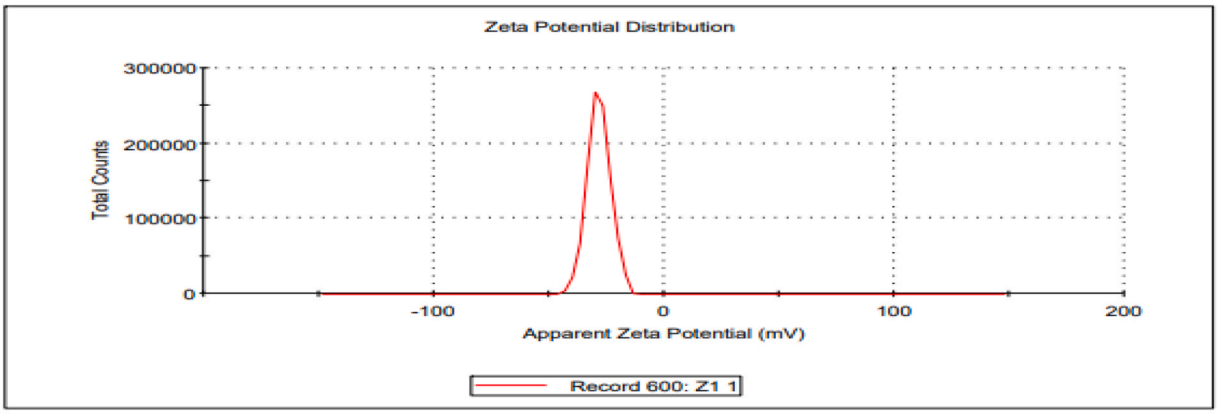


**(b):** Zeta-potential analysis of menthol crystals

**Fig. 4.** (a): Size distribution analysis of menthol crystals (b): Zeta-potential analysis of menthol crystals.

### 3.3.2. FTIR analysis of menthol crystals produced from different fractions

A comparison of FTIR analysis of standard menthol crystals with the menthol crystals produced in this study confirmed that the chemical nature of produced menthol crystals was same as that of standard menthol crystals. The spectrum in (Fig. 3a) is representative of standard menthol crystals. A strong and broad peak at 3250 $cm^{-1}$ indicated -OH stretching (H-bonded), peaks at 2721 $cm^{-1}$ and 2922 $cm^{-1}$ indicated (C-H stretching), and sharp peaks at 916 $cm^{-1}$, and 1177 $cm^{-1}$ indicated (C-O stretching) [38]. At frequencies from 1341 $cm^{-1}$ to 1446 $cm^{-1}$ menthol exhibited C-H bending typical of methyl groups present within menthol. The bands at 670 $cm^{-1}$ and 775 $cm^{-1}$ result from skeletal mode vibrations of the hexagonal ring in menthol structural unit. Similar assessments of menthol have been reported previously [39–41]. Similar spectra were recorded for menthol crystals produced from different fractions of mint oil including F1 (Fig. 3b), F2 (Fig. 3c), F3 (Fig. 3d), F4 (Fig. 3e), and F5 (Fig. 3f).

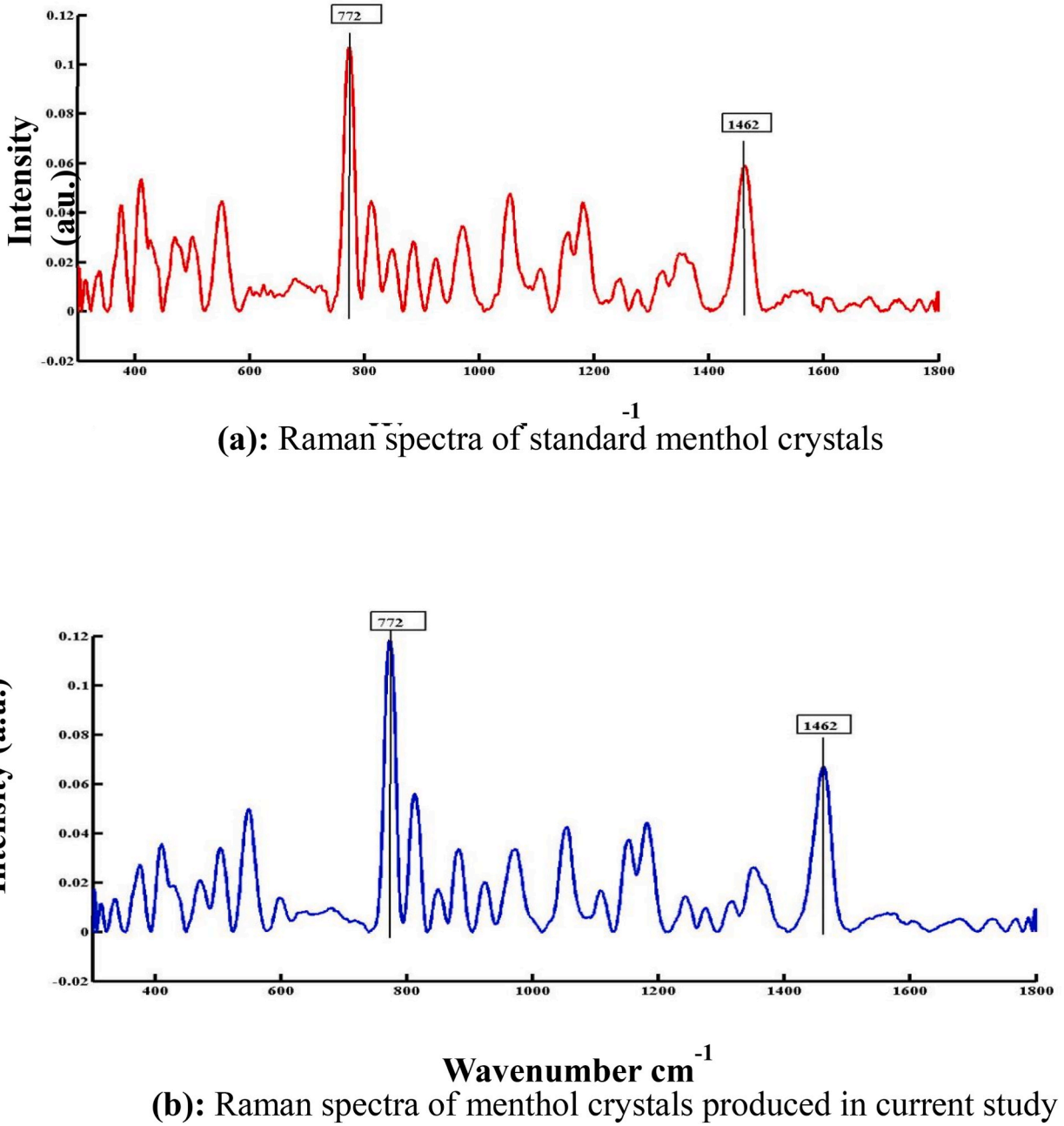


**Fig. 5.** (a): Raman spectra of standard menthol crystals (b): Raman spectra of menthol crystals produced in current study.

### 3.3.3. Zeta-sizer, particle size analysis, and zeta potential measurement of menthol crystals

*3.3.3.1. Particle size analysis of menthol crystals produced in current study.* The analysis indicated that mean diameter of menthol crystal particles was 209.5 nm. The polydispersity index (PDI) was 0.449 ± 0.9. The PDI represents the particle size distribution in system. A low PDI indicates a narrow size distribution (SD), while values higher than 0.5 indicate a very wide size distribution [42]. The PDI value in current study was lower than 0.5 which indicated the narrow size distribution of particles in the crystals. The size distribution of particles was further confirmed by zeta-potential measurements of menthol crystals (Fig. 4a).

*3.3.3.2. Zeta potential measurement of menthol crystals produced in current study.* The results presented in (Fig. 4b) showed high zeta potential values for menthol crystals. The zeta potential value of menthol crystals produced in current study was −28mV. Zeta potential of the menthol crystals produced in current study was closer to the range, which indicated the stability of the menthol crystals [43]. Previous research revealed that, the average particle size of menthol is 16 μm [35]. However, the menthol crystals produced by the spray seeding crystallization process had a much smaller average size i.e., 0.449 μm. It is well understood that high volatility of menthol and its transformation to amorphous whisker are the major obstacles for its practical application in drug delivery system. According to the earlier studies, menthol crystals after being produced through traditional crystallization processes, were further processed to micronized form using expensive chemical methods [35]. The method described in current study produced menthol crystals directly in micronized form, which is confirmed by SEM analysis, FTIR, and zeta-sizer particle size distribution analysis. The process was simple, less time consuming and cost-effective as no expensive chemicals were used in this method.

*3.3.3.3. Raman spectroscopic characterization of menthol crystals.* Raman spectroscopic analysis was also performed to confirm the identity of menthol crystals produced in this study. For standard menthol crystals, two intense peaks were recorded at 774 and 1462 $cm^{-1}$. Strong bands at 774 $cm^{-1}$ and 1462 $cm^{-1}$ were linked to the menthol ring's deformation and the CH2/CH3 bending modes of the menthol crystals, respectively (Fig. 5a). Earlier studies also reported the same results [44–46]. Almost similar results were recorded for menthol crystals produced in this study. Raman spectrum of menthol crystals produced in this study is presented in (Fig. 5b).

*3.3.3.4. XRD analysis of menthol.* The physical state of menthol was examined by x-ray diffraction method. Fig. 6 illustrate the XRD diffractograms of the standard and prepared menthol crystals. The diffraction patterns of both menthol samples exhibited several sharp peaks, indicating the crystalline nature of samples. The standard menthol sample showed well defined crystalline peaks at 2θ equals to 9°, 14.01°, 22°, 53° and 57.98° (Fig. 6a). However, the prepared menthol crystals showed well defined crystalline peaks at 2θ equals to 5.5°, 14.5°, 15°, 17.4°, 14.41°, 19°, 20° and 22.5° (Fig. 6b). The diffraction patterns of both menthol samples exhibited several sharp peaks, indicating the crystalline nature of menthol. The size of crystallites and the percentage change in the crystallite size of the menthol crystals were calculated from XRD diffraction patterns using Scherrer equation (crystallite size = $k\lambda/b\cos\theta$) and results are depicted in Tables 6 and 7. The standard sample of menthol exhibited the crystallite size of 45.08 nm (Table 6), while the crystallite size of prepared menthol was reduced to 32.3 nm (Table 7). The crystallite size of menthol was reported to be 52.23 nm in a previous study which is quite closer to the standard menthol crystals studied [47]. The crystallite size of menthol crystals prepared in the current study was significantly reduced. The reduction in particle size of menthol crystals may enhance its dissolution rate when used in various medication, food, and esthetic applications [35].

## 4. Conclusions

Different processes, including TPCP, SPMFD followed by SSC, and SC, were employed for the molecular crystallization of menthol. Among these, the (SPMFD followed by SSC) method emerged as the most effective, yielding optimal menthol crystals. We employed comprehensive characterization techniques such as scanning electron microscopy (SEM) for surface morphology, x-ray diffraction (XRD) for crystal structure and crystallite size evaluation, and FTIR and Raman spectroscopy for analyzing the chemical nature of the crystals. Additionally, measurements of particle size distribution and zeta potential were conducted. The combined results indicated a successful production of stable (−)-menthol crystals with reduced particle size. This reduction holds promise for enhancing the dissolution rate of menthol crystals, thereby expanding their applications in various fields, including pharmaceuticals, cosmetics, and health products. This study marks a significant advancement in the preparation of menthol crystals, with potential implications for diverse industries.

## Data availability

Data included in the article/supplementary material is referenced in the article.

## CRediT authorship contribution statement

**Ayesha Mushtaq:** Writing – original draft, Investigation. **Muhammad Asif Hanif:** Supervision, Data curation. **Raziya Nadeem:** Validation, Formal analysis. **Zahid Mushtaq:** Writing – review & editing, Visualization, Methodology.

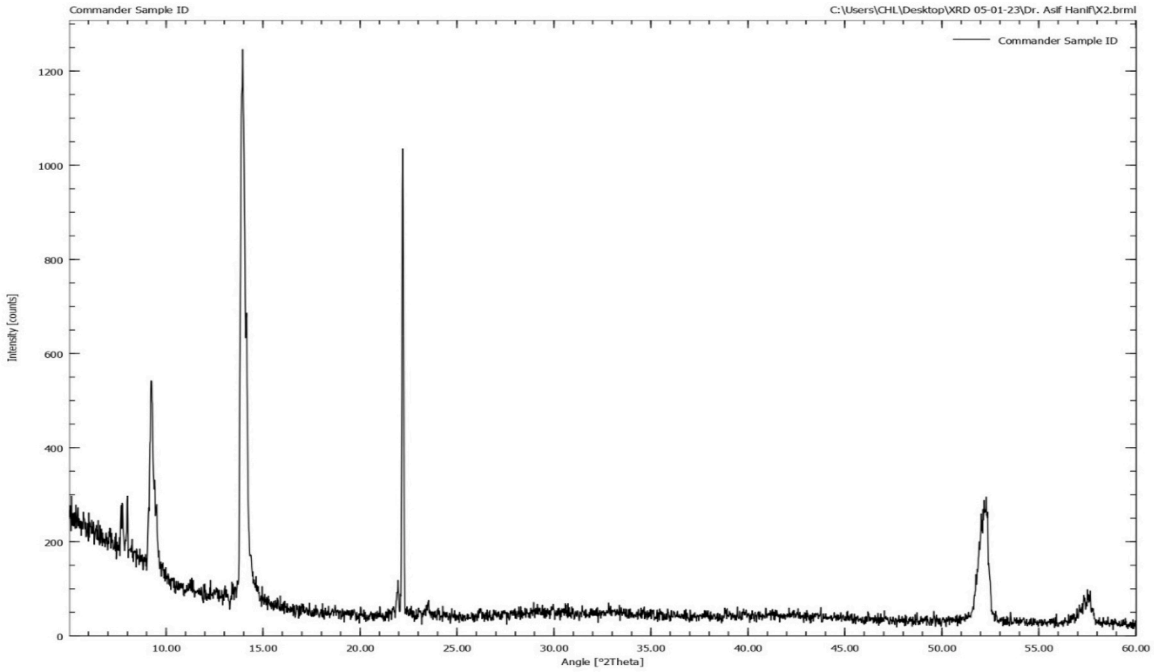


**(a):** X-ray diffraction analysis of standard menthol crystals

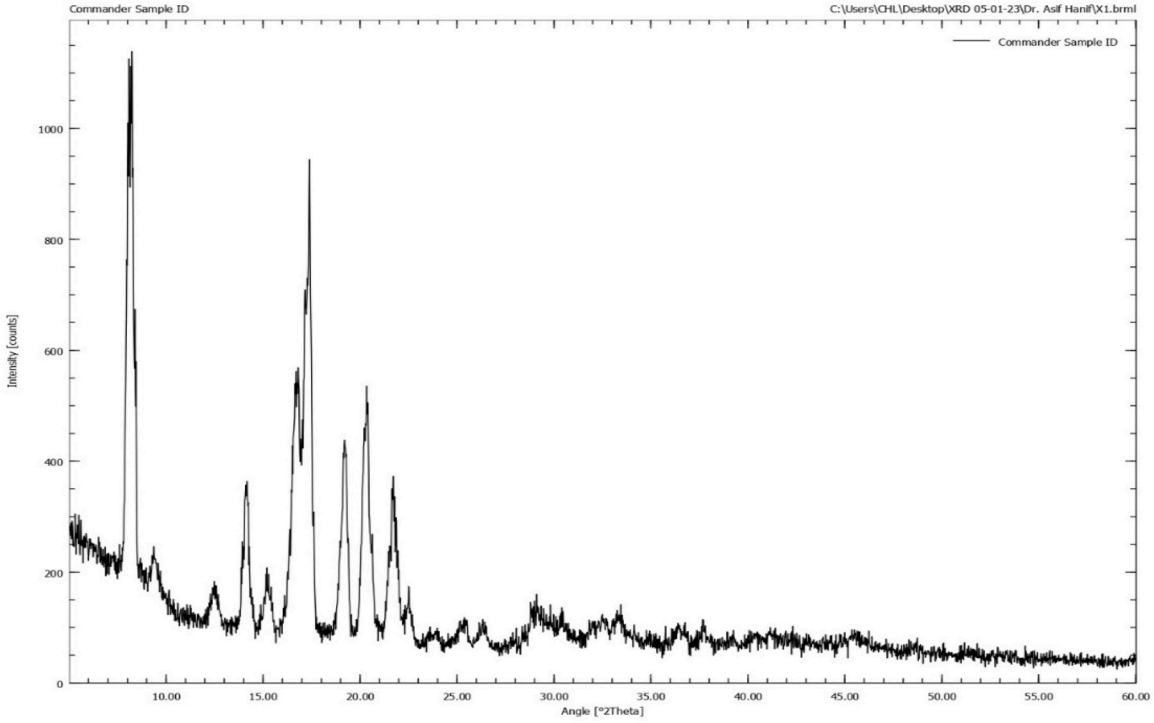


**(b):** X-ray diffraction analysis of menthol crystals produced in the current study

**Fig. 6.** (a): X-ray diffraction analysis of standard menthol crystals (b)X-ray diffraction analysis of menthol crystals produced in the current study.

**Table 6**
Detailed interpretations of XRD spectroscopic analysis of standard menthol crystals.

| Pos. [°2Th.] | Height [cts] | FWHM Left [°2Th.] | d-spacing [Å] | Rel. Int. [%] | Crystallite size D (nm) | Average crystallite size (45.08) |
|---|---|---|---|---|---|---|
| 9.24 | 388.78 | 0.16 | 9.57 | 33.78 | 50.62 | |
| 13.93 | 1150.95 | 0.19 | 6.36 | 100 | 40.6 | |
| 22.19 | 953.26 | 0.09 | 4.01 | 82.82 | 82.2 | |
| 52.26 | 240.04 | 0.24 | 1.76 | 20.86 | 37.47 | |
| 57.46 | 50.10 | 0.63 | 1.61 | 4.35 | 14.38 | |

**Table 7**
Detailed interpretations of XRD spectroscopic analysis of prepared menthol crystals.

| Pos. [°2Th.] | Height [cts] | FWHM Left [°2Th.] | d-spacing [Å] | Rel. Int. [%] | Crystallite size D (nm) | Average crystallite size (32.2) |
|---|---|---|---|---|---|---|
| 8.012 | 722.54 | 0.19 | 11.03 | 90.18 | 40.46 | |
| 14.15 | 245.17 | 0.19 | 6.26 | 30.6 | 40.68 | |
| 15.24 | 81.25 | 0.31 | 5.82 | 10.14 | 25.45 | |
| 16.76 | 427.61 | 0.31 | 5.29 | 53.37 | 25.50 | |
| 17.38 | 801.26 | 0.16 | 5.10 | 100 | 51.05 | |
| 19.21 | 344.46 | 0.27 | 4.62 | 42.99 | 29.24 | |
| 20.35 | 424.74 | 0.31 | 4.36 | 53.01 | 25.63 | |
| 21.73 | 259.01 | 0.39 | 4.09 | 32.32 | 20.55 | |

## Declaration of competing interest

The authors declare that they have no known competing financial interests or personal relationships that could have appeared to influence the work reported in this paper.

## References


[1] A. Gupta, et al., Genetic variability and correlations of essential oil yield with agro-economic traits in Mentha species and identification of promising cultivars, Ind. Crop. Prod. 95 (2017) 726–732.
[2] R. Nowak, et al., Menthol-containing Solids Composition, Google Patents, 2013.
[3] R. Tardugno, et al., Phytochemical composition and in vitro screening of the antimicrobial activity of essential oils on oral pathogenic bacteria, Nat. Prod. Res. 32 (5) (2018) 544–551.
[4] A.A. Alves, et al., Mentha arvensis IN OIL SOLID-LIQUID EQUILIBRIUM, Braz. J. Chem. Eng. 36 (2019) 609–614.
[5] I.-L. Gatfield, et al., Process for the Preparation of L-Menthol, Google Patents, 2004.
[6] D.B. Marcum, B.R. Hanson, Effect of irrigation and harvest timing on peppermint oil yield in California, Agric. Water Manag. 82 (1–2) (2006) 118–128.
[7] C. Benedict, et al., The formation of rubber-producing cortical parenchyma cells in guayule (Parthenium argentatum Gray) by low temperature, Ind. Crop. Prod. 31 (3) (2010) 516–520.
[8] J. Asili, et al., Influence of extraction methods on the yield and chemical composition of essential oil of platycladus orientalis (l.) franco, Jundishapur J. Nat. Pharm. Prod. 2 (1) (2007) 25–33.
[9] L. Caputo, et al., Impact of drying methods on the yield and chemistry of Origanum vulgare L. essential oil, Sci. Rep. 12 (1) (2022) 3845.
[10] C. Nurhaslina, S.A. Bacho, A. Mustapa, Review on drying methods for herbal plants, Mater. Today: Proc. 63 (2022) S122–S139.
[11] M. Elyemni, et al., Extraction of essential oils of Rosmarinus officinalis L. by two different methods: hydrodistillation and microwave assisted hydrodistillation, Sci. World J. 2019 (2019).
[12] A.C. Atti-Santos, et al., Extraction of essential oils from lime (Citrus latifolia Tanaka) by hydrodistillation and supercritical carbon dioxide, Braz. Arch. Biol. Technol. 48 (2005) 155–160.
[13] S. Rezazi, S. Abdelmalek, S. Hanini, Kinetic study and optimization of extraction process conditions, Energy Proc. 139 (2017) 98–104.
[14] N.B. Syarul, et al., Analysis of the chemical composition of the essential oil of Polygonum minus Huds. using two-dimensional gas chromatography-time-of-flight mass spectrometry (GC-TOF MS), Mol 15 (10) (2010) 7006–7015.
[15] D.N. Do, et al., Fractionating of lemongrass (Cymbopogon citratus) essential oil by vacuum fractional distillation, Process 9 (4) (2021) 593.
[16] R.N. Almeida, R.d.P. Soares, E. Cassel, Fractionation process of essential oils by batch distillation, Braz. J. Chem. Eng. 35 (2018) 1129–1140.
[17] F. Zhang, et al., Progress and opportunities for utilizing seeding techniques in crystallization processes, Org. Process Res. Dev. 25 (7) (2021) 1496–1511.
[18] A. Borba, A. Gómez-Zavaglia, Infrared spectroscopy: an underexploited analytical tool for assessing physico-chemical properties of food products and processing, Curr. Opin. Food Sci. (2022) 100953.
[19] J. Kameda, et al., Morphological analyses of minute crystals by using stereo-photogrammetric scanning electron microscopy and electron back-scattered diffraction, J. Microsc. 228 (3) (2007) 358–365.
[20] M.A. Hanif, et al., Raman spectroscopy for the characterization of different fractions of hemp essential oil extracted at 130 C using steam distillation method, Spectrochim. Acta A Mol. Biomol. 182 (2017) 168–174.
[21] M.A. Hanif, et al., Evaluation of the effects of Zinc on the chemical composition and biological activity of basil essential oil by using Raman spectroscopy, Ind. Crops Prod. 96 (2017) 91–101.
[22] F. Astutiningsih, et al., Optimization of saffron essential oil nanoparticles using chitosan-Arabic gum complex nanocarrier with ionic gelation method, Int. J. Food Sci. 2022 (2022).
[23] M.K. Makkar, S. Sharma, H. Kaur, Evaluation of Mentha arvensis essential oil and its major constituents for fungitoxicity, J. Food Sci. Technol. 55 (9) (2018) 3840–3844.
[24] Y. Kohari, et al., Hydrodistillation by solvent-free microwave extraction of fresh Japanese peppermint (Mentha arvensis L.), J. ESSENT. OIL BEAR PL. 23 (1) (2020) 77–84.
[25] T. Bui-Phuc, T. Nhu-Trang, N. Cong-Hau, Comparison of chemical composition of essential oils obtained by hydro-distillation and microwave-assisted extraction of Japanese mint (Mentha arvensis L.) grown in Vietnam, in: IOP Conf. Ser. Mater. Sci. Eng., IOP Publishing, 2020.
[26] S. Hazrati, et al., Effect of harvesting time variations on essential oil yield and composition of Sage (Salvia officinalis), Horticulturae 8 (2) (2022) 149.
[27] M. Nadeem, et al., Processing and quality evaluation of menthol mint oil, Int. j. math. stat. invent. 5 (2) (2017) 68–70.
[28] M. Alvi, S. Ahmad, K. Rehman, Preparation of menthol crystals from Mint (Mentha arvensis), Int. J. Agric. Biol. 3 (4) (2001) 527–528.

[29] K.L. Waters, G.D. Beal, Some physical and chemical properties of commercial racemic menthol, J. Am. Plann. Assoc. 34 (2) (1945) 52–56.
[30] D. Lawrence, B. Cadman, A.C. Hoffman, Sensory properties of menthol and smoking topography, Tob. Induc. Dis. 9 (1) (2011) 1–8.
[31] E.J. Krüsemann, et al., The sensory difference threshold of menthol odor in flavored tobacco determined by combining sensory and chemical analysis, Chem. Senses 42 (3) (2017) 233–238.
[32] Z. Czégény, et al., Thermal behaviour of selected flavour ingredients and additives under simulated cigarette combustion and tobacco heating conditions, J. Anal. Appl. Pyrolysis 121 (2016) 190–204.
[33] C. Turek, F.C. Stintzing, Stability of essential oils: a review, Compr. Rev. Food Sci. Food Saf. 12 (1) (2013) 40–53.
[34] M. Tortello, et al., Effect of thermal annealing on the heat transfer properties of reduced graphite oxide flakes: a nanoscale characterization via scanning thermal microscopy, Carbon 109 (2016) 390–401.
[35] N. Suankaew, et al., L-Menthol crystal micronized by rapid expansion of supercritical carbon dioxide, J. Ind. Eng. Chem. 18 (3) (2012) 904–908.
[36] Z. Huang, et al., Formation of ultrafine aspirin particles through rapid expansion of supercritical solutions (RESS), Powder Technol. 160 (2) (2005) 127–134.
[37] S.A.F.a.S. Muhammad, et al., A novel method for the production of crystalline micronised particles, J. Med. Plants Res. 388 (1–2) (2010) 114–122.
[38] B. Athokpam, S.G. Ramesh, R.H. McKenzie, Effect of hydrogen bonding on the infrared absorption intensity of OH stretch vibrations, Chem. Phys. 488 (2017) 43–54.
[39] H.H. Ali, et al., New insight into single phase formation of capric acid/menthol eutectic mixtures by Fourier-transform infrared spectroscopy and differential scanning calorimetry, Trop. J. Pharm. Res 19 (2) (2020) 361–369.
[40] F.A. Al-Bayati, Isolation and identification of antimicrobial compound from Mentha longifolia L. leaves grown wild in Iraq, Ann. Clin. Microbiol. Antimicrob. 8 (1) (2009) 1–6.
[41] H. Kadhem, H. AL-Mathkhury, Inhibitory effect of menthol extracted from Mentha rubra on methicillin-resistant Staphylococcus aureus, Worl Exp. Bioc. 3 (2) (2015) 150–154.
[42] K. Hunthayung, et al., Controlled release and macrophage polarizing activity of cold-pressed rice bran oil in a niosome system, Food Funct. 10 (6) (2019) 3272–3281.
[43] K. Wadher, et al., Influence of electrical field during crystallization on dielectric constant, zeta potential and oxidation and reduction properties of paracetamol, Drug Dev. Ind. Pharm. 46 (2) (2020) 188–191.
[44] P. Vargas Jentzsch, L.A. Ramos, V. Ciobotă, Handheld Raman spectroscopy for the distinction of essential oils used in the cosmetics industry, J. Cosmet. Sci. 2 (2) (2015) 162–176.
[45] T. Osmałek, et al., Novel organogels for topical delivery of naproxen: design, physicochemical characteristics and in vitro drug permeation, Pharm. Dev. Technol. 22 (4) (2017) 521–536.
[46] P. Vargas Jentzsch, et al., Raman spectroscopy in the detection of adulterated essential oils: the case of nonvolatile adulterants, J. Raman Spectrosc. 52 (5) (2021) 1055–1063.
[47] M.K. Trivedi, et al., Structural and physical properties of biofield treated thymol and menthol, J. mol. pharm. org. process res. 3 (2) (2015) 1000127.